Title

Role of indentation depth and contact area on human perception of softness for haptic interfaces.

Journal

Science advances, 5(8)

ISSN

2375-2548

Authors

Dhong, Charles
Miller, Rachel
Root, Nicholas B
et al.

Publication Date

2019-08-01

DOI

10.1126/sciadv.aaw8845

Peer reviewed

MATERIALS SCIENCE

Role of indentation depth and contact area on human perception of softness for haptic interfaces

Charles Dhong[1]*, Rachel Miller[1], Nicholas B. Root[2], Sumit Gupta[3], Laure V. Kayser[1], Cody W. Carpenter[1], Kenneth J. Loh[3], Vilayanur S. Ramachandran[2], Darren J. Lipomi[1]*

In engineering, the "softness" of an object, as measured by an indenter, manifests as two measurable parameters: (i) indentation depth and (ii) contact area. For humans, softness is not well defined, although it is believed that perception depends on the same two parameters. Decoupling their relative contributions, however, has not been straightforward because most bulk—"off-the-shelf"—materials exhibit the same ratio between the indentation depth and contact area. Here, we decoupled indentation depth and contact area by fabricating elastomeric slabs with precise thicknesses and microstructured surfaces. Human subject experiments using two-alternative forced-choice and magnitude estimation tests showed that the indentation depth and contact area contributed independently to perceived softness. We found an explicit relationship between the perceived softness of an object and its geometric properties. Using this approach, it is possible to design objects for human interaction with a desired level of perceived softness.

INTRODUCTION

In the engineering sciences, "softness" is associated with deformability. A material is determined to be soft due to some combination of low elastic modulus, low stiffness, and high ductility. The tactile cues governing the human perception of softness, however, are less straightforward to identify (*1*). It has been suggested that the indentation depth (the distance that a fingertip penetrates into an object) (*2*–*4*) and contact area (the interfacial area between a fingertip and object) (*5*–*7*) are important tactile cues. The indentation depth and contact area are generated simultaneously during touch, making it difficult to decouple the two parameters. Intentional design of materials and devices for generating tactile sensation—such as haptic displays and human-machine interfaces—requires understanding the role of and relationship between indentation depth and contact area (*8*, *9*). Here, our goal was to decouple these parameters using a system that allowed human subjects free exploration of a variety of engineered elastomeric slabs. These slabs were designed to produce precise ratios between the indentation depth and contact area at a given force, which decoupled the two parameters. Decoupling was possible using combinations of Young's modulus, slab thickness, and micropatterning of relief structures (pits) on the surface. Using these engineered elastomeric slabs in human subject tests, we quantified how the indentation depth and contact area affected the perception of softness. These results can help design more realistic tactile interfaces in electronic skin for instrumented prostheses, soft robotics, and haptics (*10*).

BACKGROUND

The perception of softness arises from both the tactile and kinesthetic senses. Afferent nerve endings in the skin give rise to the sense of touch, and those in the muscles, tendons, and ligaments give rise to a kinesthetic perception of motion or of the "solidness" of objects. Dynamic control of the perception of softness (or hardness) is achieved in haptic devices using one of several methods. For example, a soft, enclosed object filled with air can change its stiffness by means of pneumatic pressure; if filled with particles, then the object can be made stiff by removing the air (i.e., jamming) (*8*, *11*–*13*). The solidness of a virtual object can also be approximated using motors, pulleys, and hydraulic actuators to resist the motion of fingers in gloves or stirrup-like apparatuses (*14*–*17*). These approaches are thus adept at producing a sense of softness based on the kinesthesia, i.e., bulk deformability. This approach stands in contrast to one that attempts to produce a dynamic sense of softness at the fingertips by manipulating near-surface properties. To achieve this goal, the relative importance of parameters such as surface porosity (i.e., integrated contact area) and Young's modulus, along with the stiffness (i.e., the extrinsic property that depends on the geometry of the object), must be established.

Understanding how the mechanical properties of solid objects influence the perception of softness has been the subject of several investigations (*2*, *6*, *12*, *18*–*21*). However, a clear picture has yet to emerge from this work because both tactile cues believed to be important in the perception of softness (i.e., indentation depth and contact area) are affected simultaneously by the mechanical properties (e.g., Young's modulus, stiffness). In a critical review, Gerling *et al.* (*20*) found several instances in which the relationships between the mechanical properties of test objects and the participant's responses to them were unclear. In some studies, it was difficult to connect participant responses with mechanical properties because of the unreliable control over the mechanical properties of samples (*20*). In other instances, some studies were regarded as ambiguous because it was assumed that controlling the intrinsic mechanical properties would automatically control the extrinsic properties such as the indentation depth and contact area on the finger (*20*). These extrinsic properties also depend on the geometry of the specimen—especially its thickness—which ultimately determines the stiffness (i.e., compliance) under bending or compression.

Hypothesizing that the indentation depth and contact area were important tactile cues in the perception of softness, several authors have taken the step of fixing either one of these two parameters (*3*, *5*–*7*, *19*, *22*). In one approach, these variables are controlled using

[1]Department of NanoEngineering, University of California, San Diego, 9500 Gilman Drive, Mail Code 0448, La Jolla, CA 92093-0448, USA. [2]Department of Psychology, University of California, San Diego, 9500 Gilman Drive, Mail Code 0109, La Jolla, CA 92093-0109, USA. [3]Department of Structural Engineering, University of California, San Diego, 9500 Gilman Drive, La Jolla, CA 92003-0085, USA.
*Corresponding author. Email: cdhong@udel.edu (C.D.); dlipomi@eng.ucsd.edu (D.J.L.)

mechanical apparatuses (*3*, *5*–*7*). These devices, however, substantially restrict the participant's movement, and thus, this setup does not resemble the way in which humans engage with objects in the real world (*19*, *22*). In another approach, mechanical apparatuses have been combined with some level of materials control, e.g., tuning the Young's modulus of the material. For example, Moscatelli *et al.* (*5*) controlled the indentation depth using an apparatus that limited how far a participant's finger could penetrate into an object. Using this approach, the authors presented test participants with two materials of the same shape but with different Young's moduli. The authors found that participants were able to determine the difference between the two materials even while restricting the indentation depth of the finger. As the indentation depth was controlled, the contact area was the only mechanical stimulus that could have affected the perception of softness (*5*). Developing a general relationship (i.e., one that is not dependent on a restrictive apparatus) between the perceived softness of samples for a range of indentation depths and contact areas, however, requires a third approach. In this approach, used here, the indentation depth and contact area at a given force are varied simultaneously using only the material so that the participants could freely interrogate the samples—i.e., without the use of physical restraints. Our central hypothesis was that the contact area and indentation depth combine in some way that determines the human perception of softness and that the functional form of this relationship can be found by independent manipulation of the modulus, thickness, and effective surface area of a set of elastomeric slabs.

The indentation depth and contact area between a finger and an object are described by the Hertzian contact model (*23*). When a finger is pressed into an object from a direction normal to the surface of the object, the finger and object deform in proportion to the Young's modulus (E) of the object and finger, the applied force (F), and the geometries of both the object and finger. The finger indents the object by a distance known as the indentation depth, δ. Simultaneously, the interfacial area between the finger and object spreads with a contact area of πa^2. Even with a light touch, the contact area encompasses a large proportion of the fingertip (*15*, *24*). This large contact area may seem problematic because the Hertzian model assumes that these deformations are relatively small. However, despite the relatively large contact area of the indenter (i.e., the finger) encountered in human touch, the Hertzian contact model has been successfully used as a first-order approximation in many studies on the tactile sense (*6*, *7*, *12*). An important consequence of the Hertzian model is that, for most elastic objects thicker than a few millimeters, it is not possible to tune the ratio between the indentation depth and contact area. This ratio remains the same even with different values of Young's modulus.

To overcome the coupling between indentation depth and contact area, we exploited a phenomenon arising from solid mechanics, along with standard techniques of microfabrication. First, we exploited the fact that a thin material (defined as an object that has a thickness similar to the expected indentation depth) becomes effectively stiffer than a thicker counterpart due to a confinement effect (*24*). This effect occurs because a thin material is immobile at the interface where it meets the rigid substrate. At large displacements, the thin, confined material becomes substantially more rigid than its bulk. Thin objects with a lower Young's modulus can be stiffer (e.g., a smaller indentation depth for a given applied force) than a thick object with a higher Young's modulus. We were thus able to "dial in" a specified relationship between indentation depth and contact area, independent of Young's modulus. Second, we were able to reduce the contact area between a slab and a finger by micropatterning relief structures (either pillars or pits) into the surface of the slab. These features reduced the effective surface area by preventing the finger from making contact with the deeper level of relief. With microstructured slabs, an important design consideration was to minimize confounding variables, e.g., inadvertent enhancement of adhesion (*25*), increased deformability of the slab by collapsing or buckling (*26*, *27*), or perception of the microstructures by the participant as texture (*28*, *29*).

By controlling the thickness and effective surface area of elastomeric slabs, we were able to tune the indentation depth and contact area of the slabs independently. These slabs were freely explored by human subjects without relying on restrictive apparatuses. In our experiments, which involved nine slabs differing on the basis of thickness, microstructuring, and Young's modulus, we asked participants to perform two psychophysical tasks: two-alternative forced-choice (i.e., which of two slabs is softer?) and magnitude estimation (i.e., rank the relative softness of all nine slabs by placing them along a scale of 1 to 10).

EXPERIMENTAL RATIONALE AND THEORY

Hertzian contact model

The indentation depth and contact area between two objects are related to the Young's modulus of a slab, the physical dimensions of both the slab and the finger, and the applied force. This relationship, described by a Hertzian contact model of an elastic sphere in contact with a semi-infinite (i.e., sufficiently thick) planar substrate (see Fig. 1A), is given as (*24*)

$$F = \frac{16Ea^3}{9R} \tag{1}$$

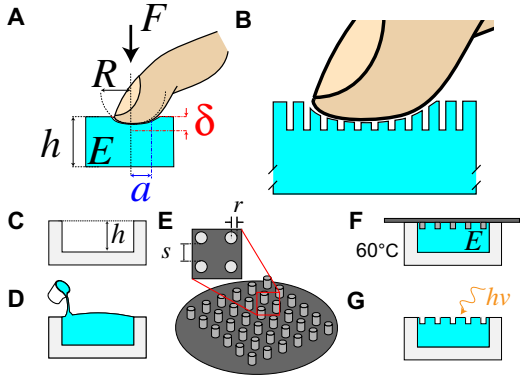

Fig. 1. Overview of experimental approach and fabrication scheme. (**A**) Hertzian contact model of a finger of radius, R, presses with a force, F, into a deformable slab with Young's modulus, E, and a controlled thickness, h. This pressing action displaced the interface between both objects by an indentation depth, δ. The finger and the slab shared an interface with a contact area of πa^2. (**B**) The creation of pits in the surface of the slab by micropatterning reduced the contact area between the finger and the slab. (**C**) The thickness of the slab, h, was controlled by cutting a pocket into an acrylic substrate to a depth equal to h. (**D**) The acrylic substrate served as a mold for a liquid PDMS prepolymer. Before curing, a micropatterned (or planar) wafer (**E**) was placed on top of the uncured PDMS (**F**). The micropatterned pillars had a radius, r, and were spaced by a distance, s. The Young's modulus, E, was controlled by the prepolymer/cross-linker ratio of the prepolymer. (**G**) The slab was exposed to ultraviolet (UV)/ozone to minimize surface viscoelasticity.

where F is the applied force, E is the Young's modulus, R is the radius of the finger, and a is the contact radius. For a rigid sphere, the contact radius, a, is geometrically related to the indentation depth by $a = \sqrt{R\delta}$. Here, E is equivalent to E_{eff}, the effective Young's modulus which for the finger (E_F) and substrate (E_S) moduli, given as

$$E_{eff} = \left(\frac{1-\nu_F^2}{E_F} + \frac{1-\nu_s^2}{E_S}\right)^{-1} \quad (2)$$

where ν is the Poisson ratio. The consequence of finite thickness is that a thin slab is effectively stiffer (i.e., a smaller displacement for a given force) than a thick slab. Assuming a similar correction factor between flat and spherical indenters, as noted by Shull *et al.* (*24*), Eq. 1 is modified as follows

$$F = \frac{16Ea^3}{9R}\left(1 + 0.15\left(\frac{a}{h}\right)^3\right) \quad (3)$$

where h is the thickness of the film. Equation 3 reverts to Eq. 1 when the thickness of the film becomes much larger than the contact radius. The indentation depth in thin films is given as

$$\delta = \left(0.4 + 0.6\ \exp\left(-1.8\frac{a}{h}\right)\right)\frac{a^2}{R} \quad (4)$$

Equations 3 and 4 show how the thickness of a film, h, is used to tune the indentation depth and contact area, which is not possible in thick films (Eq. 1).

Slab thickness

Equation 4 demonstrates how the thickness of the slab affects the ratio between the contact radius and the indentation depth. Using a microCNC (computer numerical control) end mill with approximately micrometer resolution, we fabricated acrylic molds by cutting circular pockets of a precise depth (h; Fig. 1C) and a fixed radius into acrylic blocks, which determined the thickness of the poly(dimethylsiloxane) (PDMS) slab (see Fig. 1D).

Avoidance of unwanted effects from microstructures

In our experimental design, we were cognizant of the fact that micropatterned structures at the surface might themselves deform in ways that could affect the perception of softness. Since the only aspect of the microstructures we were interested in was their effect on the surface area presented to the fingertip, it was possible to make the relief structure very shallow (10 μm). We thus designed the height of the features such that bending or buckling would be a very small fraction (i.e., <1%) of the total deformation of the slab (*26*, *27*, *30*). Our calculations are shown in the Supplementary Materials. In short, the deformation of the relief structures is negligible if the participants apply a downward force with a deviation within 30° of perpendicular. Moreover, this calculation is independent of Young's modulus and downward force (*26*). This analysis was performed for the microstructured slabs with an effective surface area of 30% (in which the raised portions were micropillars). Microstructured slabs with an effective surface area of 50% were formed instead by fabricating wells, i.e., the inverse of pillars because of ease of fabricating the silicon mold by photolithography.

In addition to inadvertently increasing deformability, patterned microstructures can enhance adhesion under certain conditions (*25*, *31*, *32*), which we were concerned might interfere with the participants' perception of softness. The patterned microstructures here, however, were of too low of a density to enhance adhesion (*33*).

We were also aware that the patterned microstructures might be perceived as a texture (a scenario we wanted to avoid). It has been shown that participants are sensitive to features much smaller than the ones used here (*28*, *29*). In those studies, however, perception of texture was found to arise from the friction forces generated by sliding a finger across a surface (*32*, *34*). These friction forces are minimized when participants tap or press into an object (i.e., no sliding). We observed that the participants always explored the slabs using a tapping or pressing motion, although they were neither told to avoid sliding their fingers nor instructed to tap. Even in a tapping mode, humans still have the ability to perceive features on a surface. We believe that it is unlikely that the participants could have perceived the individual microstructures, as humans have static two-point discrimination of features around 1.7 mm when sensed at the fingertips (*35*). This two-point resolution is much larger than the size (r = 20 μm) and pitch of the microstructures in the slabs.

Young's modulus

Assuming two slabs with identical thicknesses, an increase in the Young's modulus decreases both the indentation depth and contact area at a given applied force of a hemispherical indenter. For two slabs with different thicknesses, however, Eq. 4 shows that the Young's modulus alone does not determine the indentation depth. In other words, stiffness (an extrinsic property) and the Young's modulus are not interchangeable terms. We thus hypothesized that it would be possible to construct a slab perceived as hard (by tuning the indentation depth via the thickness), although it was constructed of material with a relatively low Young's modulus.

The slabs were constructed from a silicone elastomer—PDMS (SYLGARD 184, Dow Corning)—and casted in acrylic molds. The Young's modulus of PDMS was controlled by the ratio of base to cross-linker. We note that the viscoelasticity of the native surface of PDMS could be perceived by participants as "stickiness." This viscoelastic adhesion was minimized by exposing the slabs to ultraviolet (UV)/ozone (Fig. 1G)—a long-lasting treatment that partially cross-links the surface and reduces tack. (*36*)

Notes on psychophysical experiments

While it is possible to monitor the interface between a finger and a substrate in real time with only a modest burden on participants (*34*, *37*), we chose not to do so. Real-time measurements, on their own, cannot determine the precise moment in which human subjects formulate their perception of softness. Instead, we designed our experiments for unobtrusiveness and free exploration. Doing so also allowed us to test a larger number of samples than would have been possible if we had increased the complexity of our experimental design to allow for real-time measurements.

We minimized potential errors from free exploration with two precautions. First, each participant was presented the slabs in a different order. We performed this randomization to reduce possible effects arising from experience or fatigue. Second, we took the statistical significance of all findings to be at a level of $P < 0.001$, which is more stringent than the commonly accepted threshold of $P < 0.05$. To support the reproducibility of the effects we observed, we repeated the

psychophysical tests and analysis approximately 1 year later on a second set of slabs with an additional 10 participants (fig. S7).

RESULTS

Designing slabs using Hertzian contact

On the basis of a Hertzian contact model, a participant might perceive a slab with a higher Young's modulus as softer than a slab with a lower Young's modulus if the latter slab was sufficiently thin. Figure 2A shows that a thin slab (<1 mm) with a low Young's modulus has a smaller indentation depth and contact area than a thicker slab with a high Young's modulus for an applied force of 1 N. For example, we compare the indentation depth of a slab with E_s = 0.1 MPa and a film thickness of 0.25 mm with a slab with E_s = 0.8 MPa with a film thickness of 3 mm. In this example, the slab with a smaller indentation depth has, by definition, a higher stiffness than the other slab with a higher Young's modulus. If a slab that is perceived as soft is also made with a low Young's modulus, then it is possible to misattribute perceived softness with a low Young's modulus. Therefore, we intentionally fabricated slabs that might be perceived as among the softest with an intermediate Young's modulus, as opposed to a low Young's modulus (the parameters used to calculate Fig. 2 are in table S1).

The downward force used by participants as they interrogated the slabs varied during the course of the psychophysical tests. This variability could have led to scenarios in which two different slabs generated identical values of indentation depth or contact area during exploration. For example, Fig. 2B shows that a large force on a thin slab or a light force on a thick slab results in identical values of the contact area (a similar scenario occurs for the indentation depth). This coincidence is potentially problematic for two reasons: (1) Two different slabs may generate the same indentation depth or contact area, and (2) the value or values of the indentation depth and contact that form the basis for the participants' responses are unknown.

Regarding (1), similar values in the contact area or indentation depth between two slabs are predicted to occur only for a narrow range of forces. Moreover, there are no two slabs that produce the same value of both indentation depth and contact area, even if the (static) force on each slab is different. This statement is verified as follows. Figure 2C is a plot showing, as a function of force, how much the ratio of indentation depth to contact area decreases between two slabs having differences in thickness in increments of 0.1 mm, given that the slabs have the same Young's modulus (i.e., the difference in the ratio of two slabs that vary in thickness by 0.1 mm). Figure 2C demonstrates that this ratio is both nonzero and nonparallel at all forces. This fact has two consequences. First, there is no single force where both the indentation depth and contact area are identical between two slabs. Second, in the event that under two different forces, this ratio is identical between two slabs, the incremental increase in indentation depth and contact area will be the same between two slabs. However, as both slabs would have had different initial values of indentation depth and contact area, the end result is that the indentation depth and contact area between both slabs will remain distinct. Although Fig. 2C has only been shown for differences in film thickness, film thickness is the most stringent slab parameter. In practice, differences in Young's modulus result in even larger differences in the ratio (between the growth of indentation depth and contact area with force) between two slabs.

Regarding (2), it may be impossible to know which combination or combinations of indentation depth and contact area formed the basis of the participants' determination of softness. Furthermore, participants used a wide range of forces during exploration, and it was important that the forces used in our model were similar to those produced by the participants. Rather than compelling the participants to press with a set force, we calibrated the forces used in our models by asking them to press on a sample placed on a scale. The range of forces we obtained, 0.1 to 3 N, was consistent with forces used in previous studies (*20*, *37*). Later, we performed analysis of participant responses on all forces within this range, and we used the force that best predicted their responses.

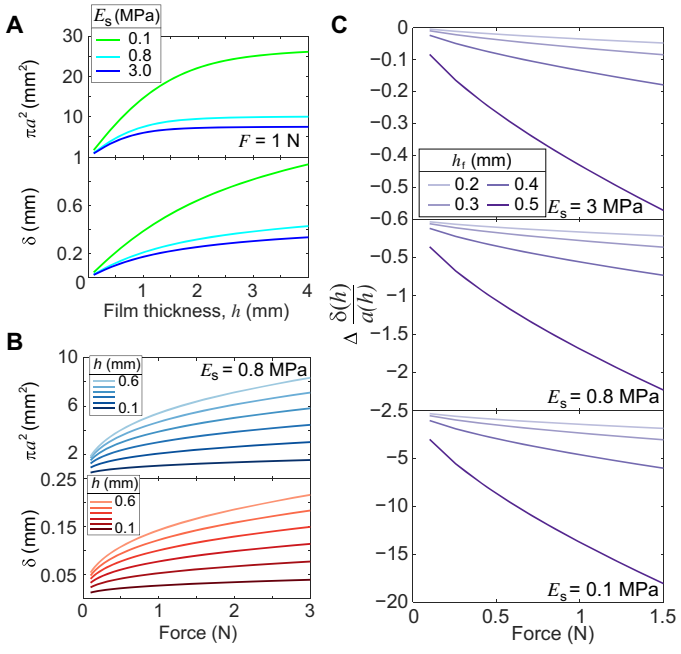

Fig. 2. Computed indentation depth and contact area of thin PDMS slabs. (**A**) The contact area (πa^2) and indentation depth (δ) as a function of slab thickness (h) and Young's modulus (E_s) for an applied force of 1 N. (**B**) Contact area and indentation depth as a function of force for a slab with a Young's modulus of 0.8 MPa. Results are obtained from Eqs. 2 to 4. (**C**) Differences in the ratio of indentation depth to contact radius between two slabs that differ in thickness by 0.1 mm as a function of force. The thicker of the two slabs has a slab thickness of h_f. Negative values indicate that thinner films have larger ratios of δ/a.

Choice of slab parameters and verification

Under Institutional Review Board (IRB) guidelines, participants must be able to perform the psychophysical tasks within a reasonable time. Participants took approximately 1 hour to perform the two-alternative forced-choice test on nine samples, which we deemed to be a reasonable duration (the addition of even a single slab would have increased the number of head-to-head comparisons from 36 to 45, increasing testing duration by 25%). Therefore, we designed slabs with the goal of efficiency, i.e., to explore the largest parameter space based on three parameters: Young's modulus, thickness, and effective surface area. We maximized the parameter space by designing each slab to vary in at least two parameters, as opposed to a single parameter. We also avoided designing sets of slabs that would have interrogated effects similar to those explored by others (such as investigating the role of Young's modulus in determination of softness of bulk, planar samples) (*20*). The Young's modulus, thickness, and effective surface area are independent parameters, which simplified the multidimensional analysis of our results. Furthermore, the Young's moduli used here span a similar range with

Table 1. Slab parameters.

Slab		Young's modulus *E* (MPa)	Thickness *h* (mm)	Effective surface area (% of original surface area)	Marker
Dark red	(**dkR**)	3.0	4.20	30	▲
Red	(**R**)	3.0	1.40	30	▲
Light red	(**ltR**)	3.0	0.60	50	★
Dark blue	(**dkB**)	0.8	0.58	100	●
Blue	(**B**)	0.8	0.50	100	●
Light blue	(**ltB**)	0.8	0.30	100	●
Dark green	(**dkG**)	0.1	0.40	30	▲
Green	(**G**)	0.1	0.20	50	★
Light green	(**ltG**)	0.1	0.13	100	●

other investigations on the perception of softness, and the increased stiffness in thin films was modest—even the thinnest slab did not exceed the stiffness of bulk slabs with a Young's modulus in the upper end of this range. (*20*)

A table of slabs used in this study is shown in Table 1, with representative images shown in Fig. 3A. We name the slabs using a code in the text and using markers in the plots. The naming convention is as follows: The darkness within each color category increases with thickness, the color (red, blue, and green) corresponds to a Young's modulus (red, highest; green, lowest), and the number of "points" on the marker corresponds with percent coverage (triangle, 30%; star, 50%; circle, unpatterned).

We measured the contact area for both a gloved finger and a rigid [poly(methyl methacrylate) (PMMA)] hemispherical indenter with a radius of 5 mm and an applied mass of 100, 200, or 300 g onto a slab using electrical impedance tomography (EIT; see Fig. 3B). This technique measures the spatially resolved deformation of the slab by monitoring differences in conductance of a piezoresistive film (<10 μm) on the surface of the slab (*38*). Figure 3B shows that the deformation of the slab (dkG) increases with applied force. That is, contact areas of 20.0, 30.4, and 48.0 mm^2 are generated using applied masses of 100, 200, and 300 g, respectively. These values are similar to those obtained in the literature (*15*, *20*, *37*). We found that the deformable finger and the rigid indenter resulted in similar contact areas with the slab.

We measured the indentation depth of the same rigid hemispherical indenter at various applied masses using a noncontact linear displacement sensor (see Fig. 3C). We achieved good agreement between our measurements (solid markers) and predictions based on Eqs. 3 and 4 (dashed lines) of indentation depth at various applied forces. At higher forces, the prediction overestimated the deformation. This overestimation is known to occur when the deformation of the slab is very large (*39*). In addition, Fig. 3C emphasizes the importance of the film thickness on the indentation depth. Although the dkR slab had a higher Young's modulus (3 MPa), it is less stiff (i.e., larger indentation depth) than the two slabs (B and ltB) with a lower Young's modulus of 0.8 MPa.

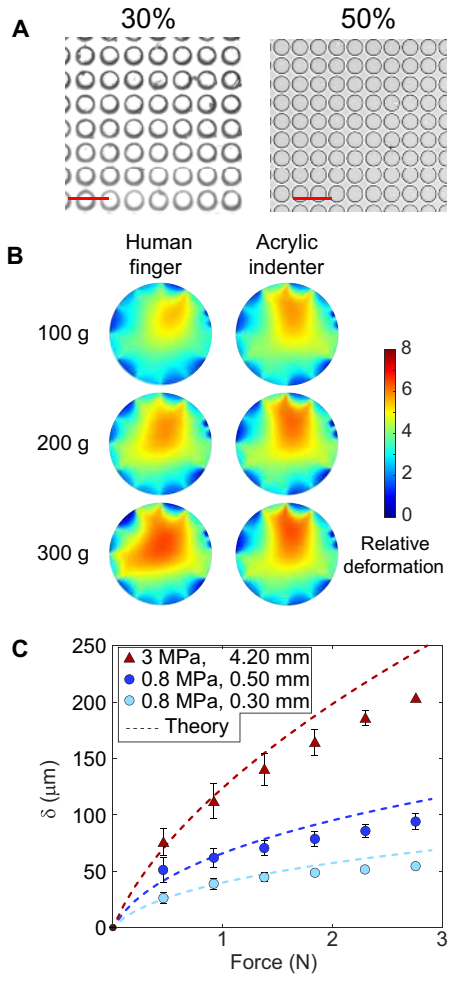

Fig. 3. Properties of PDMS slabs. (**A**) Optical images of the microstructured slabs. Patterned microstructures reduce the effective contact area to either 30 or 50% of the original area. Scale bars, 100 μm. (**B**) Electrical impedance tomography (EIT) of a finger and acrylic indenter to visualize the contact area with different applied masses. The color is proportional to the displacement. (**C**) Measurements of indentation depth of an acrylic indenter on slabs that vary in the Young's moduli or slab thickness.

The two-alternative forced-choice test

The percentage of times a slab was judged by participants as softer than all other slabs ("aggregate percentage") is shown in Fig. 4A and the individual head-to-head comparisons are in Fig. 4B. Although only two slabs were presented at a time, participants consistently judged some slabs as softer than others. Some of these judgments matched expectations from a Hertzian contact model. For example, ltR (E = 3.0 MPa; h = 0.60 mm; effective surface area, 50%) has the lowest aggregate percentage. Therefore, ltR was perceived as the least soft (i.e., the "hardest") slab. The perception of ltR as the hardest slab matches expectations because ltR was thin and has the highest Young's modulus. Other results did not match expectations suggested by Hertzian contact. For example, dkB (E = 0.8 MPa; h = 0.58 mm; effective surface area, 100%) has the highest aggregate percentage (it was perceived as the softest slab). Although we expected that this slab would be among the softest due to its large thickness and unpatterned surface, it had an intermediate Young's modulus.

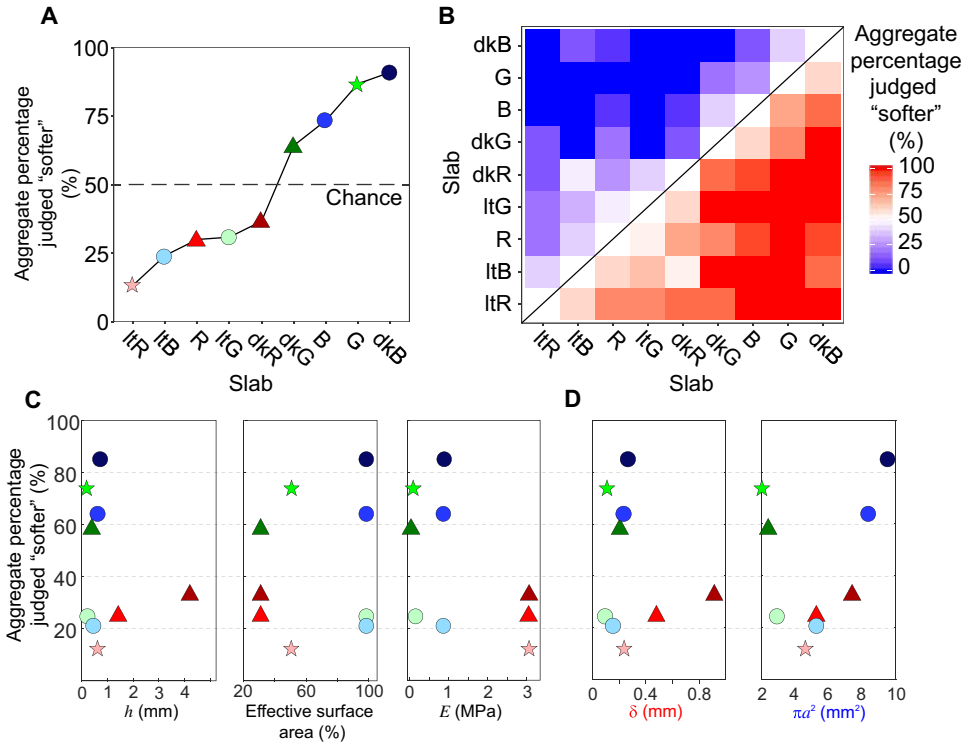

Fig. 4. Results of the two-alternative forced-choice test. (**A**) Aggregate percentage of times a slab was judged as the softer slab compared to the other slabs. The line is to guide the eye. (**B**) This plot is a sample-by-sample, head-to-head comparison, in which the slabs are arranged in the rows and columns by increasing aggregate percentage. The color of each square quantifies whether a sample on the *x* axis was judged as softer than a sample on the *y* axis. (**C**) Aggregate percentage of times a slab was judged as the softer slab as a function of intrinsic slab parameters: thickness, effective surface area, and Young's modulus. (**D**) Same as (C) but as a function of extrinsic parameters (i.e., those produced as a result of contact with an indenter): indentation depth and contact area. Indentation depth and contact area are calculated for $F = 1$ N, a representative force used for the purpose of plotting. Marker shape represents extent of micropatterning (effective surface areas: triangles, 30%; stars, 50%; circles, 100%), color represents Young's modulus, and shade represents relative thickness (darkest is the thickest, within each color group). Error bars are excluded because the aggregated data ignore sample-by-sample trends. Data represent a total of 540 individual comparisons between five participants ($n = 5$).

The aggregate percentage is a convenient visualization of the head-to-head comparisons. However, plotting the data this way can obscure trends that are present in head-to-head comparisons. The following case illustrates consistency in the conclusions that can be drawn from the way that these data are visualized. As can be seen in Fig. 4A, R and ltG have a similar aggregate percentage. Examination of the head-to-head comparison in Fig. 4B reveals that participants had difficulty deciding which slab was softer—R was judged as softer than ltG in about half of all trials (8 of 15). Furthermore, R and ltG also performed similarly when compared to other slabs (shown by the similarity of color intensity between rows R and ltG in Fig. 4B). In another case, however, similar values of the aggregate percentage did not correspond to similar head-to-head comparisons. In this example, ltB and ltG scored similarly by aggregate percentage, but the head-to-head comparison reveals that each performed differently when compared to a third slab. When compared to dkR, participants judged ltB to be softer than dkR 47% of the time, whereas ltG was judged to be softer than dkR 27% of the time. Therefore, the aggregate percentage visualizes certain trends that are not apparent in the head-to-head comparisons and vice versa.

Although the aggregate percentage and head-to-head comparisons do not always recapitulate the same trends, participants responses show a remarkable consistency between the two. To visualize this consistency, we have organized the head-to-head comparisons in Fig. 4B and the slabs according to an increasing aggregate percentage. By doing so, one can see that there are no red boxes above, or blue boxes below, the diagonal in Fig. 4B. This partitioning means that the ranking of softness based on an aggregate percentage results in the same order as a ranking based on head-to-head comparisons. Consistency between aggregate percentage and head-to-head comparisons is not guaranteed to occur in two-alternative forced-choice tests: Mozart may be thought to be the greatest composer of the classical era from a large number of head-to-head comparisons, but perhaps Beethoven "always beats" Mozart and no one else (see the Supplementary Materials for an elaborated counterexample involving the "best" songs). For example, dkG has the fourth highest aggregate percentage, which means that there are three slabs softer than dkG. On the basis of an aggregate percentage, the three slabs that are the softer than dkG are B, G, and dkB (Fig. 4A), which are also the same three slabs that were softer than dkG in head-to-head comparisons (i.e., raw data in Fig. 4B). Note that this conclusion is valid regardless of the order of slabs in Fig. 4B. The only potential inconsistency between the aggregate and head-to-head data is between R and ltG. Overall, ltG was judged as softer by an amount of 0.8% more often than R, but in head-to-head comparisons, R was perceived as softer than ltG 53% (8 of 15) of the time. This comparison represents one anomaly in the set of 540 total comparisons (a success rate of 99.8%) and is well within the margin of error. Rather than an inconsistency, participants likely considered both R and ltG as equally soft.

Consistency between the aggregate percentage and the head-to-head comparisons is remarkable because it means that the perception of softness is "transitive" in the mathematical definition. Transitivity means that if sample A is softer than sample B and B is softer than C, then A should be perceived as softer than C. Transitivity has several important implications for human perception (*40*). It implies that softness is a measurable quantity or variable within tactile perception, which has not been previously established. Transitivity also implies that the stimulus under investigation—the perception of softness—is evaluated by humans on a univariate scale. Evidence for a univariate scale of softness is emphasized by our earlier finding where two slabs differing in every physical property (R and ltG) were perceived as equally soft. In that situation, multiple physical properties are synthesized into a single (univariate) representation of perceived softness. A univariate scale also implies that the scale for judging softness is consistent between participants and that the perception of softness is a basic sensation (*40*). That is, the perception of softness is not composed of a combination of more basic sensations. We note that, while the perception of softness might not be composed from more basic components, this is distinct from the mechanical definition, in which softness is determined by a combination of the Young's modulus and slab geometry.

Finding that the perception of softness is transitive is not an artifact of the two-alternative forced-choice test. Unlike other psychophysical tests (such as magnitude estimation, which we performed next), a two-alternative forced-choice test does not compel participants to evaluate softness along a single dimension. Moreover, participants were not trained to interpret softness along a single dimension because the two-alternative forced-choice test was performed before magnitude estimation for all participants.

We plotted the aggregate percentage judged softer for each slab against five different parameters in Fig. 4, C and D: thickness (h), effective surface area (%), Young's modulus (E), indentation depth (δ), and contact area (πa^2). Thickness, effective surface area, and Young's modulus are properties of the slab (Fig. 4C), while indentation depth and contact area emerge only upon contact with the finger (Fig. 4D). The principal conclusion from this representation is that no single property of the slab nor aspect of deformation was by itself an accurate predictor of softness. For example, it is tempting to conclude from the leftmost plot of Fig. 4C that perceived softness correlated with increased thickness (considering the red and blue series representing constant Young's modulus). All other parameters being equal, this expectation would have been valid. However, a closer inspection reveals a complex interplay of parameters. For example, in the red series, the two triangles were perceived as softer than the star, although the triangles represent slabs with the smallest effective surface area (which we hypothesized would have been perceived as the least soft). Moreover, the green series (representing the lowest Young's modulus) follows a trend that is completely the opposite of expectations, with the unstructured slab (the circle) being judged the least soft, although it has the largest contact area. This defiance of expectations pervades the relationships plotted in Fig. 4, C and D. This apparent complexity points to the need for a model, which accounts for all parameters native to the slab, and incorporates the simultaneous effects of indentation depth and contact area due to the downward force of the finger.

Hertzian contact model that best predicts human responses

A lack of clear trends in participant responses with either indentation depth or contact area led us to hypothesize that the perception of softness depends on both factors. We determined the optimal relationship between the perception of softness, indentation depth, and contact area by considering three interconnected scenarios. First, the indentation depth and contact area of each slab grows differently with increasing applied force (see Fig. 2), and thus, the predictive power of each model may depend on the force. Second, the finger may be better modeled as a rigid object, although the finger is deformable, because human subjects may unconsciously account for the deformability of their fingers. Third, the indentation depth and contact area may contribute to the perception of softness equally (as suggested by Hertzian contact) or unequally.

For each variation of the three interconnected scenarios, a Hertzian contact model generated a set of the indentation depths and contact areas for the nine slabs. These sets of indentation depth and contact area are then connected to participant responses using a Bradley-Terry model (*41*)—a widely used model in psychology to predict the outcome of paired comparisons. We quantified the ability of each variation of these Hertzian contact models to predict participant responses using an Akaike information criterion (AIC) (*42*) in Fig. 5. An AIC quantifies the predictive power of different Hertzian contact models by estimating how much information (defined in dimensionless units of the logarithm of "likelihood") is gained or lost with each Hertzian contact model (*42*). Lower values of the AIC indicate that one model is more predictive than another model. The magnitude that one model is

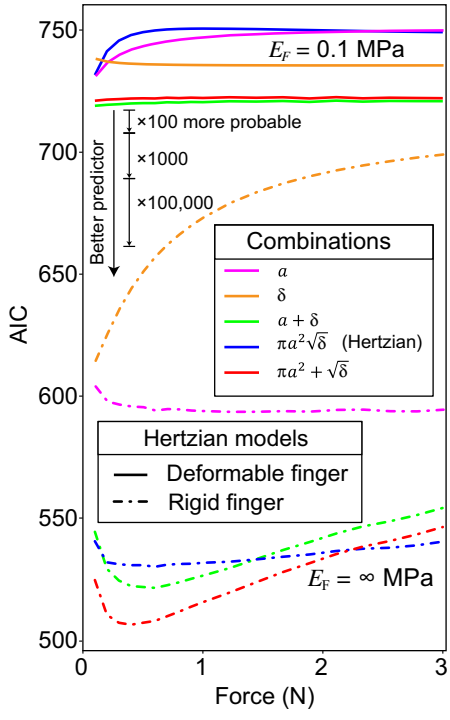

Fig. 5. Comparison of models that best relate human perception of softness to the indentation depth and contact area in a two-alternative forced-choice test. The predictive power, based on the AIC (lower values are better predictors), is shown at different applied forces. Two Hertzian models are shown (dashed and solid lines) where the finger is treated as a "deformable finger" (E_F = 0.1 MPa) and a "rigid finger" (E_F = ∞). Five different combinations of indentation depth, δ, and/or contact radius, a, are shown. The scale bar denotes a 100-fold increased probability of a model fitting the data from an incremental change in AIC. The scale bar can be translated along the y axis, but a linear increase in the distance represents an exponential increase that a scenario is more probable.

more predictive than another is known as the relative likelihood. We calculate the increased relative likelihood of one model over another by taking the differences in AIC between two models. Large differences in AIC indicate that the model with the lower AIC is much more predictive than the other model. While differences in AIC are important, the absolute value of AIC has no meaning. The end goal of this analysis is to identify the scenario with the lowest AIC and therefore best predicts participant responses. A flowchart of this analysis is provided in fig. S2.

All the dashed lines in Fig. 5 have a lower AIC than the solid lines, which indicates that participant responses are better predicted by a Hertzian contact model that considers the finger as a rigid object, although, in reality, the finger is deformable. The models that consider the finger as a rigid object always obtained a better fit (comparing lines of the same color in Fig. 5), regardless of the applied force or the different methods of combining indentation depth and contact area. One explanation is that participants may compensate (in the brain, as opposed to mechanically at the finger) for the deformability of their finger during exploration of the slab. Modeling the finger as a rigid object improves the prediction of participant responses by a large amount, as shown by a reduction in the AIC by nearly 200 points. As the AIC is logarithmic with probability, a difference of 200 points represents a probability increased by 2.7×10^{43} (calculated by $e^{200/2}$) that a model is a better fit. For reference, a difference of 10 points in AIC is typically sufficient to establish significance that one model is more predictive (*42*). The best fit is obtained at a force of around 0.4 N, which is approximately the force at which the largest differences (the steepest slope) in indentation depth and contact area are present (Fig. 2B). This result supports the findings of Park *et al.* (*19*) that the fingers were most sensitive to changes in softness when the indentation depth of a slab was changed rapidly. These experiments were conducted by immobilizing the finger of a participant between a static support and a contacting plate containing a deformable material. The velocity with which the contacting plate pressed into the finger was controlled using a motor (*19*).

Our results support that the contact area is a tactile cue (*5*). A model that considers the indentation depth alone (Fig. 5, orange line) has reduced predictive power (by a factor of 5×10^{21}). This finding suggests that studies that investigate either compliance (the axial displacement for a given force) or haptic devices that modulate softness by depressing a rigid surface with varying spring constants may only be valid at the given contact area of the test-specific apparatus. Limiting validity to a given contact area is particularly restrictive because most objects simultaneously change in both the indentation depth and contact area during touch. A parallel conclusion is valid for the role of indentation depth on the perception of softness (Fig. 5, magenta line). Knowing that both the indentation depth and contact area are important, there are two possibilities for combining the indentation depth and contact area.

A multiplicative combination of the contact area multiplied by the square root of the indentation depth (Fig. 5, blue line) performs well, but it is not the best model because it does not generate the lowest AIC. Further substitutions of $a = \sqrt{R\delta}$ performed worse. Although at higher forces, the AIC of the blue line is lower than the red line, there is no guarantee that participants that used these high forces to determine softness and the minimum AIC, regardless of force, are the best predictor. The best combination for the rigid finger was by adding the contact area to the square root of the indentation depth. This was also the best combination, regardless of modeling the finger as rigid or deformable. This combination also preserves the exponent relationship between the contact radius and indentation depth as inspired by Hertzian contact (i.e., taking the relationship of $a = \sqrt{R\delta}$ and substituting this relationship into a^3, which leads to $a^2 + \sqrt{\delta}$, $a + \delta$, etc.). We also considered the contact radius plus the indentation depth (Fig. 5, green line) because the contact radius and indentation depth have consistent dimensions, but this generated a poor fit.

There are several alternative models that one could propose for predicting participant responses. These models vary on the basis of exponential power, consideration of the finger as rigid or deformable, or ignoring or including the effect of the patterned microstructures. These alternative models (fig. S3) did not perform as well as the ones included in Fig. 5. For example, excluding the reduced contact area from the patterned microstructures reduced the predictive power by a factor of 10^8.

The fact that an additive model best explained participant responses suggests that the act of pressing a finger into a deformable surface generates two distinct tactile cues for perceiving softness—although the act is one physical event. In vision, there is precedence for this division of perceptual cues from a single physical input, such as the distinct sensations of "colorfulness" and "saturation" (*43*), which are both derived from a single physical property—the wavelength of light. Using the Bradley-Terry model with the lowest AIC (the best fit model), it was found that the indentation depth and contact area are both statistically significant predictors of participant performance ($P < 0.001$ at $F = 0.3$ N for both coefficients, McFadden's pseudo-$r^2 = 0.28$). The probability of judging slab 1 as softer than slab 2 is calculated by

$$\text{Probability of slab 1 softer than slab 2} = \frac{e^{\lambda_1 - \lambda_2}}{1 + e^{\lambda_1 - \lambda_2}}$$
$$\lambda_i = 503\ [\mathrm{m}^{-\frac{1}{2}}]\sqrt{\delta_i} + 1.10 \times 10^6\ [\mathrm{m}^{-2}]\pi a_i^2 \quad (5)$$

One method of validating Eq. 5 is to redo the analysis based on the responses from four participants and use this equation to predict the results of the fifth participant. Known as a "leave-one-out cross-validation" (*44*), data from four participants predict the responses of the fifth with an average accuracy of 78.3% (fig. S5). We performed the same analysis on a second dataset involving a similar set of slabs and 10 additional participants (fig. S7).

Solving the nonlinear system of Eqs. 5 and 6 with Eqs. 3 and 4 yields the probability of perceiving one slab as softer than another due to the slab thicknesses, Young's moduli, and effective surface area. Assuming two sufficiently thick slabs, the minimum difference in the Young's modulus required for participants to detect a difference in softness with a 95% success rate is given as

$$0.95 = \frac{e^G}{1 + e^G}$$
$$G = \left(\frac{9RF}{16}\right)^{\frac{1}{3}}\left(\left(\frac{503}{\sqrt{R}}\right)\left(E_1^{-\frac{1}{3}} - E_2^{-\frac{1}{3}}\right) + 1.104 \times 10^6 * \left(\frac{9RF}{16}\right)^{\frac{1}{3}}\left(E_1^{-\frac{2}{3}} - E_2^{-\frac{2}{3}}\right)\right) \quad (6)$$

The contact area—as manipulated by micropatterned relief structures—was found to be an important tactile cue despite the fact that, anatomically, the spacing of the relief features is smaller than that

of the mechanoreceptors in the finger. We rationalize this apparent incongruity in the following way: Contact with the micropatterned surface creates a heterogenous strain field to a depth within the skin that lies within the receptive field of mechanoreceptors (fig. S4) (*45*). Grant *et al.* (*46*) has found in studies of distinguishing raised patterns of dots through touch that humans are sensitive to tactile stimuli with a greater resolution than suggested by the density of the sensory neurons, a phenomenon known as "hyperacuity." This phenomenon is well known in other areas of human perception. For example, in the science of vision, hyperacuity has been demonstrated by the ability of participants to resolve dots that are spaced more closely than one might expect from the density of light-sensitive cells in the eye (*47*).

We further elaborate on exactly what we mean by contact area, since its definition is critical in determining how humans may use this parameter to form a perception of softness. Geometrically, there are two methods of reducing the contact area. The first method is simply to create a smaller "footprint," the roughly circular area of contact between the slab and the finger. The second is to keep the footprint constant but to remove some portions of contact within this footprint. Micropatterning does the latter. The finding that participants were sensitive to micropatterning suggests that there must be some mechanism by which participants determine a true contact area, perhaps by sensing that some regions of the skin are in and out of contact with the surface (again, possibly through the effect of micropatterning on the heterogeneous strain field that penetrates into the skin; fig. S4). An alternative hypothesis of perceiving softness might say that humans are sensitive only to the radius of contact without regard to the integrated, "true," contact area within the footprint. This mechanism would perhaps be simpler physiologically because determining a radius only requires two points, whereas determining the true contact area requires more. Nevertheless, we believe that this "two-point" or "radial" hypothesis is unlikely based on our experimental design. That is, our results predict that micropatterned slabs are perceived to be less soft than planar slabs even if the footprint of contact with the finger (and thus the contact radius) is identical.

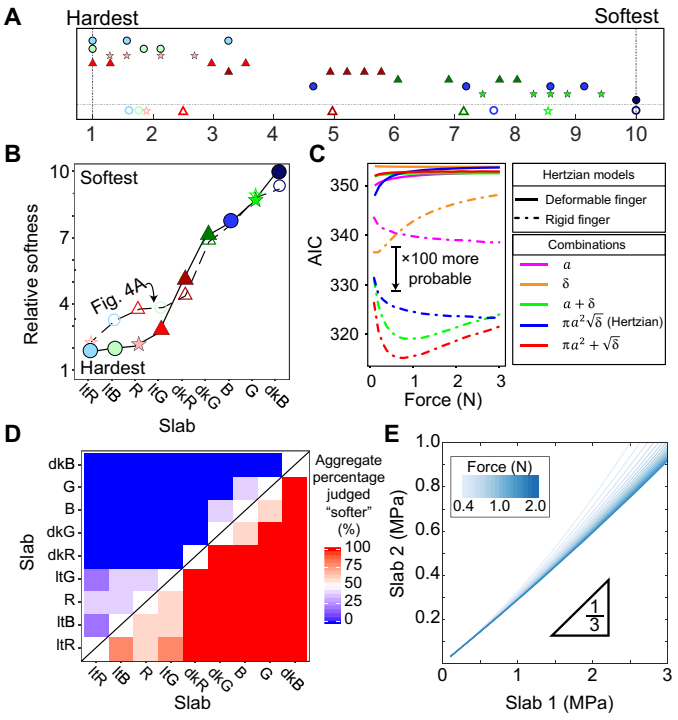

Fig. 6. Results of the magnitude estimation test. (**A**) Participants ($n = 5$) ranked slabs on a numerical scale of perceived softness, where the distance between slabs indicated relative levels of perceived softness. A "1" indicated the hardest sample and a "10" represented the "softest" sample. Hollow symbols at the bottom represent average values; solid markers represent participant responses. Slabs were judged on a scale of 1 to 10 with 33 discrete locations. (**B**) Participant response on the number line test as compared to a two-alternative forced-choice test. (**C**) Predictive power of different Hertzian models and combinations of indentation depth and contact area. The scale bar denotes a 100-fold increased probability of a model fitting the data from an incremental change in AIC. A linear increase in the differences in AIC between two models represents an exponential increase in probability. (**D**) Individual, head-to-head comparisons from the magnitude estimation test. (**E**) Curve representing the ratio between the Young's modulus of two slabs so that slab 2 feels twice as soft as slab 1. Slab 1 is shown for different Young's moduli (Eq. 8) and at applied forces similar to human touch.

Magnitude estimation test

In addition to the two-alternative forced-choice test—which established how likely a participant was to perceive one slab as softer than another—we also asked that they perform a magnitude estimation test. In this test, we asked the same participants to place the same nine slabs on a single number line with a simplified scale of 1 to 10, 10 representing the softest slab. For increased resolution, the actual scale contained 33 discrete positions on which the participants were instructed to rank the slabs. We instructed that the spacing between the slabs was representative of how much softer—or harder—each slab was compared to the one next to it. The results of this magnitude estimation test are shown in Fig. 6.

In Fig. 6A, the relatively narrow range of slab placement between participants indicates that the perception of softness is consistent between individuals. For example, all five participants perceived ltG to be between 1 and 2 on the scale, and most considered dkR to be between 5 and 6.

A comparison between both psychophysical tests (in Fig. 6B) shows relatively good agreement in the order of slabs from hardest to softest, supporting the robustness of both the tests and the sample set. We overlay participant responses on a numerical scale (filled markers, solid line) with the previous two-alternative forced-choice study (open markers, dashed line). Note that the y axis is not directly comparable between tests and instead highlights the order of slabs by softness. There are small discrepancies for the exact order of ltB, ltR, R, and ltG in terms of relative softness, although participants in both tests perceived those slabs as among the hardest slabs.

Using data from both the two-alternative forced-choice and magnitude estimation tests, we evaluated the hypothesis that slabs, which were perceived to be more similar in softness (magnitude estimation test), were also more difficult to distinguish from one another (two-alternative forced-choice test). Although this analysis may seem redundant, there was no guarantee that the way in which participants conceived of "softness" was consistent between the two tests. That is, the idea of softness could have meant something different to participants depending on whether the slabs are presented two at a time or all nine at once. We found a statistically significant correlation between the difference in relative softness between two slabs and the frequency of picking one of the two slabs as the softer one ($r = 0.73$, $t = 6.15$, $P < 0.001$). That is, if one slab was consistently found to be softer than another slab in the two-alternative forced-choice test, then those two slabs were also likely to be far apart on the 1 to 10 scale. This result, combined with the consistency between

both tests in Fig. 6B, suggests that participants are using the same conception of softness in both psychophysical tests.

Earlier, a variation of the Hertzian contact model ($\pi a^2 + \sqrt{\delta}$, with a rigid finger) best explained the two-alternative forced-choice test (Fig. 5). The same variation of the Hertzian contact model also best explains the magnitude estimation data (as shown by AIC in Fig. 6C). Note that the absolute value of the AIC cannot be used between two different psychophysical tests. We confirmed the same three findings as earlier. First, the best-fit model is one that considers a finger as a rigid object. Second, both the indentation depth and contact area are important contributors to perceptions of softness. Last, adding the contact area with the square root of the indentation depth provided the best fit out of all tested combinations. In the magnitude estimation test, the best fit occurs at a slightly higher force of 0.6 N.

Results from the magnitude estimation test support the transitive property of softness. As magnitude estimation does not provide paired comparisons, we created an analog of a paired comparison by placing all results according to the best model we identified from Fig. 6C. This analog considers a slab to be "judged softer" if the slab was placed higher on the number line. Transitivity is preserved within this test, as shown in Fig. 6D by the lack of red boxes above (or blue boxes below) the black diagonal line. As stated previously, magnitude estimation already forces participants to evaluate softness along a single axis. Therefore, magnitude estimation can only support, but not prove, that the perception of softness is transitive.

Using the best-fit linear model at 0.6 N, we found that the coefficients for both indentation depth and contact area are statistically significant predictors of participant performance ($P < 0.001$ for both coefficients, $r^2 = 0.61$). The softness is calculated as follows

$$\text{Softness} = -8.4 + 1127[\text{m}^{-\frac{1}{2}}]\sqrt{\delta} + 1.84 \times 10^6[\text{m}^{-2}]\pi a^2 \quad (7)$$

We formulated Eq 7 to range from 1 to 10. A value of 1 indicates a very thin slab at 3 MPa, and a value of 10 represents a thick slab at 0.8 MPa. The range of softness encompassed by Eq. 7 and in this study is relevant to many haptic devices and previous studies on the perception of softness (*20*). Equation 7 can be modestly extrapolated outside a scale of 1 to 10, but future research is needed to determine the extent of this extrapolation. One possibility is that an intercept of −8.4 represents a lower limit to the perception of softness and objects harder than −8.4 may be difficult for participants to distinguish. The ability of Eq. 7 to predict participant responses is quantified using a leave-one-out cross-validation. The data from four participants predicted the responses of the fifth participant with an average error of 1.59 on a 10-point scale (fig. S6). These findings were supported by performing the same analysis using a similar but different set of slabs with 10 additional participants (fig. S7).

Combining Eq. 7 with a Hertzian contact model provides prediction about how the physical dimensions of a slab that feels twice as soft as another slab. For example, if considering a sufficiently thick slab (Eq. 1), then Eq. 7 estimates the properties of another slab that is twice as soft. Thin substrates—roughly estimated as <5 mm for Young's moduli above 100 kPa—require substituting Eqs. 3 and 4 into Eq. 7 and solving the implicit equation

$$2 = \frac{-8.4 + \left(\frac{9FR}{16E_1}\right)^{\frac{1}{3}}\left(\frac{1127\ \text{m}^{-\frac{1}{2}}}{\sqrt{R}} + 1.84 \times 10^6\pi\ \text{m}^{-2}\left(\frac{9FR}{16E_1}\right)^{\frac{1}{3}}\right)}{-8.4 + \left(\frac{9FR}{16E_2}\right)^{\frac{1}{3}}\left(\frac{1127\ \text{m}^{-\frac{1}{2}}}{\sqrt{R}} + 1.84 \times 10^6\pi\ \text{m}^{-2}\left(\frac{9FR}{16E_2}\right)^{\frac{1}{3}}\right)} \quad (8)$$

Assuming $F = 1$ N and a finger radius of 5 mm, Eq. 8 shows that a thick, unpatterned slab with $E = 300$ kPa is perceived to be twice as soft as a thick slab made with $E = 1$ MPa. A plot of Young's moduli of a given slab (slab 1) and the Young's moduli of a second slab (slab 2) that will be perceived as twice as soft as the original slab is shown in Fig. 6E. For a range of Young's moduli from 100 kPa to 3 MPa and for a range of forces that approximate human exploration, an approximately threefold reduction in the Young's moduli is necessary to fabricate a slab that feels twice as soft as the original slab.

DISCUSSION

In this study, we performed psychophysical testing with engineered elastic slabs to explore the human perception of softness. These slabs allowed participants to move freely during testing, which closely mimicked how humans explore surfaces in real life. We have four key findings that are important for engineering haptic interfaces: (i) We identified two new strategies for tuning the perceived softness of an object. Reducing the effective surface area in contact with the finger, through micropatterning, and reducing slab thickness both reduced the perceived softness of an object. (ii) We found that the indentation depth and contact area are both important parameters for humans when determining the perceived softness of an object. Therefore, controlling the perception of softness by altering the indentation depth (i.e., compliance or stiffness) may not achieve the desired change in perceived softness if the contact area is ignored and vice versa. (iii) We found explicit relationships between the perception of softness and the slab parameters, such as the Young's modulus, thickness, and surface coverage. These equations can be used to recreate different magnitudes of softness in artificial objects or to predict a success rate in perceiving one object as softer than another. (iv) We found that the perception of softness exists on a univariate scale. This suggests that tactile devices are able, in principle, to recreate intermediate values of softness between two extremes. It also suggests that haptic devices generate the same increased relative softness for multiple users or equivalently for a single, recurring user.

This study also demonstrated five conclusions that may inform basic studies on the sense of touch. (i) The indentation depth and contact area form independent tactile stimuli. These two tactile stimuli are then combined, at an unknown junction between mechanical transduction and conscious perception, into a univariate representation of softness. (ii) Participant behavior was best predicted when we ignored the deformability of the finger and considered it as rigid. This result suggests that humans may compensate for the deformability of their own fingers when judging the softness of objects. (iii) The perception of softness is a basic component in tactile perception—as opposed to a combination of more fundamental components—because it exists on a univariate scale. (iv) Participants are not sensitive to the Young's modulus directly. Rather, they are sensitive to the deformation on the finger, which depends on the geometry of the slab and the Young's modulus. (v) The human perception of softness is better predicted by considering the total area of contact, as opposed to the radius of contact. This distinction suggests that information from several mechanically sensitive neurons is integrated to measure an area, whereas a radius only requires a measurement of the distance between two neurons. Together, these findings could lead to improved design of human-machine interfaces such as prostheses and electronic skin and could potentially inform basic studies on the sense of touch.

MATERIALS AND METHODS

Slab fabrication

Slabs were made by end-milling (Minitech CNC; ~1-μm XYZ resolution) a circular pocket with a diameter of 2.5 cm into acrylic squares with dimensions of 3 cm by 3 cm to a depth ranging from 140 to 400 μm. These pockets were filled with a PDMS prepolymer. The PDMS prepolymer was mixed and degassed before pouring. Excess PDMS was squeezed out by placing a silicon wafer flush against the acrylic square. Before casting, the silicon wafer was spin-coated with a thin (≪1 μm) layer of 5% (w/w) PMMA/anisole at 2000 rpm to form a release layer. This acrylic-PDMS prepolymer–silicon wafer construct was then cured at 60°C for 1 hour in an oven to cross-link the elastomer. Micropatterned features were fabricated into PDMS by replica molding. PDMS slabs were cured against micropatterned wafers (see the "Micropatterning silicon wafers" section for procedure for micropatterning). Slabs that did not require micropatterning were molded against an unpatterned (smooth) silicon wafer to ensure a consistent level of roughness between all slabs. The Young's modulus of the PDMS was controlled by mixing different prepolymer base: cross-linker ratios. We fabricated slabs using PDMS mixed at ratios of 5:1, 12:1, and 30:1 (base to cross-linker) and measured the Young's moduli of 3.12 ± 0.11 MPa, 0.75 ± 0.05 MPa, and 0.11 ± 0.01 MPa respectively, using a uniaxial tensile test (Mark-10, Instron). These moduli are referred to as 3, 0.8, and 0.1 MPa, respectively. Slabs were then exposed to UV/ozone (NovaScan) for 4 hours to permanently remove any adhesive tack from PDMS (*36*).

Micropatterning silicon wafers

Silicon wafers were micropatterned using SU-8 2007 (MicroChem), an epoxy-based photocurable negative-tone photoresist. Silicon wafers were cleaned using acetone, isopropyl alcohol, and deionized water and baked for 10 min at 200°C. A 10-μm-thick layer of SU-8 2007 was deposited onto the wafers by spinning at 1500 rpm, with its thickness verified by white-light interferometry (F20, Filmetrics). Following a preexposure bake at 95°C for 3 min, wafers were exposed to I-line UV (EVG620, EV Group) with a mylar photomask (Fineline) at 140 mJ/cm^2. Wafers were then postexposure baked at 95°C for 3 min, developed using an SU-8 developer (MicroChem), and then hard-baked at 200°C for 10 min. We controlled the contact area by decreasing the spacing between circles (s = 24 and 8.7 μm to achieve 30 and 50% of the original contact area, respectively). To avoid fabricating features that were too delicate for use as a mold, the slabs patterned to achieve 30% of the original contact area were composed of individual pillars extending from the surface, whereas the slabs patterned to achieve 50% were composed of an inverse of pillars—a series of wells. These wells are less susceptible to undesirable modes of deformation because they are formed by a single, contiguous network of features, whereas pillars are individual, stand-alone features. Last, to maintain a similar nanoscale roughness between microstructured and flat slabs, both microstructured and flat slabs were cured against the polished surface of a silicon wafer.

Calibration of indentation depth

The indentation depth was measured as a function of the applied load using a noncontact, capacitive displacement sensor (LD701-5/10, Omega). The voltage of the sensor is proportional to the distance to a metal target. We thus attached a metal target to a plastic, hemispherical indenter (radius, 5 mm) and applied various loads onto the indenter. The displacement sensor was calibrated using a manual z-stage with a micromanipulator (Newport).

Electrical impedance tomography

EIT creates a two-dimensional (2D) spatial map of conductivity by measuring the voltage of an array of electrodes placed at the boundary of a piezoresistive film. This piezoresistive film was made from multiwalled carbon nanotubes mixed with latex, which was deposited on the surface of the slabs through spray coating. The relative thinness of the piezoresistive film does not appreciably interfere with the mechanical response of the slabs. Along the periphery of the piezoresistive film, 12 equidistant electrodes were attached. At each electrode, direct current was applied while the voltage was being measured. The voltage measurements, using Newton's one-step error reconstruction algorithm, produced a 2D map of conductivity. The 2D map of conductivity is directly proportional to the strain due to a piezoresistive film. Detailed procedures are explained in a previous study (*38*).

Psychophysical tests

We conducted two psychophysical experiments to measure how human subjects' perception of softness relates to the physical properties of our slabs. In both experiments, the participants were instructed to interpret softness using their own subjective judgment. We did not define softness or give examples of soft objects. The participants were five healthy volunteers aged 19 to 31 years. All individuals participated in both experiments in the same order: two-alternative forced choice followed by magnitude estimation. All participants gave informed consent before participating, and our experimental protocols were approved by the IRB of University of California, San Diego (project #170248S). For the first experiment, we used a two-alternative forced-choice test to quantify the discriminability of the slabs. For the second experiment, we used the magnitude estimation test to quantify the subjectively experienced softness of the slabs.

Two-alternative forced-choice test

Participants sat at a desk, and a visual barrier was placed in front of the slabs. In each trial, a pair of slabs was presented to the subject. Participants were instructed to freely explore the surfaces of the slabs for as long as they wished and then indicate which slab they perceived as softer. Each of the 36 possible pairs of the nine stimuli was presented three times in randomized order (i.e., 108 trials total), and the initial location of each slab (left versus right) was randomized. This test enabled slab-by-slab comparisons and was designed to measure the effect of coupling between indentation depth and contact area on the perception of softness.

Magnitude estimation test

Participants were allowed to stand for a greater range of movement. They were instructed to place the same slabs from the two-alternative forced-choice test on a number line from 1 (softest slab) to 33 (hardest slab). The experimenter emphasized that it was important to arrange slabs closer to or further from neighboring slabs relative to how similar or different they perceived it to be. Participants could freely explore any slab at any time and could rearrange the slabs as many times as desired. The experiment ended when the participant indicated to the experimenter that the positions of the slabs matched their subjective perception of the softness of a slab.

SUPPLEMENTARY MATERIALS

Supplementary material for this article is available at http://advances.sciencemag.org/cgi/content/full/5/8/eaaw8845/DC1

Comparing the elastic energy of a single feature supported on a substrate

Hertzian contact model of a deformable finger

REFERENCES AND NOTES

1. C. Xu, Y. Wang, S. C. Hauser, G. J. Gerling, In the tactile discrimination of compliance, perceptual cues in addition to contact area are required. *Proc. Hum. Factors Ergon. Soc. Annu. Meet.* **62**, 1535–1539 (2018).
2. S. C. Hauser, G. J. Gerling, Force-rate cues reduce object deformation necessary to discriminate compliances harder than the skin. *IEEE Trans. Haptics* **11**, 232–240 (2018).
3. M. Di Luca, B. Knörlein, M. O. Ernst, M. Harders, Effects of visual–haptic asynchronies and loading–unloading movements on compliance perception. *Brain Res. Bull.* **85**, 245–259 (2011).
4. M. A. Srinivasan, R. H. LaMotte, Tactual discrimination of softness. *J. Neurophysiol.* **73**, 88–101 (1995).
5. A. Moscatelli, M. Bianchi, A. Serio, A. Terekhov, V. Hayward, M. O. Ernst, A. Bicchi, The change in fingertip contact area as a novel proprioceptive cue. *Curr. Biol.* **26**, 1159–1163 (2016).
6. G. Ambrosi, A. Bicchi, D. De Rossi, E. Scilingo, The role of contact area spread rate in haptic discrimination of softness, in *Proceedings of the 1999 IEEE International Conference on Robotics and Automation, 1999* (IEEE, 1999), vol. 1, pp. 305–310.
7. A. Bicchi, E. P. Scilingo, D. de Rossi, Haptic discrimination of softness in teleoperation: The role of the contact area spread rate. *IEEE Trans. Robot. Autom.* **16**, 496–504 (2000).
8. H. Culbertson, S. B. Schorr, A. M. Okamura, Haptics: The present and future of artificial touch sensation. *Annu. Rev. Contr. Robot. Auton. Sys.* **1**, 385–409 (2018).
9. M. Fontana, E. Ruffaldi, F. Salasedo, M. Bergamasco, On the integration of tactile and force feedback, in *Haptics Rendering and Applications* (InTech, 2012), pp. 47–74.
10. F. L. Hammond, R. K. Kramer, Q. Wan, R. D. Howe, R. J. Wood, Soft tactile sensor arrays for micromanipulation, in *2012 IEEE/RSJ International Conference on Intelligent Robots and Systems (IROS)* (IEEE, 2012), pp. 25–32.
11. S. S. Robinson, K. W. O'Brien, H. Zhao, B. N. Peele, C. M. Larson, B. C. M. Murray, I. M. Van Meerbeek, S. N. Dunham, R. F. Shepherd, Integrated soft sensors and elastomeric actuators for tactile machines with kinesthetic sense. *Extreme Mech. Lett.* **5**, 47–53 (2015).
12. S. Okamoto, H. Nagano, Y. Yamada, Psychophysical dimensions of tactile perception of textures. *IEEE Trans. Haptics* **6**, 81–93 (2013).
13. Y. Visell, S. Okamoto, Vibrotactile sensation and softness perception, in *Multisensory Softness* (Springer, 2014), pp. 31–47.
14. A. Song, D. Morris, J. E. Colgate, M. A. Peshkin, Real time stiffness display interface device for perception of virtual soft object, in *2005 IEEE/RSJ International Conference on Intelligent Robots and Systems (IROS'05)* (IEEE, 2005), pp. 139–143.
15. F. Kimura, A. Yamamoto, Effect of delays in softness display using contact area control: Rendering of surface viscoelasticity. *Adv. Robot.* **27**, 553–566 (2013).
16. P. Polygerinos, N. Correll, S. A. Morin, B. Mosadegh, C. D. Onal, K. Petersen, M. Cianchetti, M. T. Tolley, R. F. Shepherd, Soft robotics: Review of fluid-driven intrinsically soft devices; manufacturing, sensing, control, and applications in human-robot interaction. *Adv. Eng. Mater.* **19**, 1700016 (2017).
17. S. Jadhav, V. Kannanda, B. Kang, M. T. Tolley, J. P. Schulze, Soft robotic glove for kinesthetic haptic feedback in virtual reality environments. *Electron. Imaging* **2017**, 19–24 (2017).
18. K. Drewing, A. Ramisch, F. Bayer, Haptic, visual and visuo-haptic softness judgments for objects with deformable surfaces, in *EuroHaptics Conference, 2009 and Symposium on Haptic Interfaces for Virtual Environment and Teleoperator Systems. World Haptics 2009. Third Joint* (IEEE, 2009), pp. 640–645.
19. J. Park, Y. Oh, H. Z. Tan, Effect of cutaneous feedback on the perceived hardness of a virtual object. *IEEE Trans. Haptics* **11**, 518–530 (2018).
20. G. J. Gerling, S. C. Hauser, B. R. Soltis, A. K. Bowen, K. D. Fanta, Y. Wang, A standard methodology to characterize the intrinsic material properties of compliant test stimuli. *IEEE Trans. Haptics* **11**, 498–508 (2018).
21. C. Cascio, F. McGlone, S. Folger, V. Tannan, G. Baranek, K. A. Pelphrey, G. Essick, Tactile perception in adults with autism: A multidimensional psychophysical study. *J. Autism Dev. Disord.* **38**, 127–137 (2008).
22. B. De Gelder, P. Bertelson, Multisensory integration, perception and ecological validity. *Trends Cogn. Sci.* **7**, 460–467 (2003).
23. J. N. Israelachvili, *Intermolecular and Surface Forces* (Academic Press, 2011).
24. K. R. Shull, D. Ahn, W.-L. Chen, C. M. Flanigan, A. J. Crosby, Axisymmetric adhesion tests of soft materials. *Macromol. Chem. Phys.* **199**, 489–511 (1998).
25. S. Das, S. Chary, J. Yu, J. Tamelier, K. L. Turner, J. N. Israelachvili, JKR theory for the stick–slip peeling and adhesion hysteresis of gecko mimetic patterned surfaces with a smooth glass surface. *Langmuir* **29**, 15006–15012 (2013).
26. L. Dies, F. Restagno, R. Weil, L. Léger, C. Poulard, Role of adhesion between asperities in the formation of elastic solid/solid contacts. *Eur. Phys. J. E.* **38**, 130 (2015).
27. C. Dhong, J. Fréchette, Peeling flexible beams in viscous fluids: Rigidity and extensional compliance. *J. Appl. Phys.* **121**, 044906 (2017).
28. L. Skedung, M. Arvidsson, J. Y. Chung, C. M. Stafford, B. Berglund, M. W. Rutland, Feeling small: Exploring the tactile perception limits. *Sci. Rep.* **3**, 2617 (2013).
29. C. W. Carpenter, C. Dhong, N. B. Root, D. Rodriquez, E. E. Abdo, K. Skelil, M. A. Alkhadra, J. Ramírez, V. S. Ramachandran, D. J. Lipomi, Human ability to discriminate surface chemistry by touch. *Mater. Horiz.* **5**, 70–77 (2018).
30. M. Lamblet, E. Verneuil, T. Vilmin, A. Buguin, P. Silberzan, L. Léger, Adhesion enhancement through micropatterning at polydimethylsiloxane–acrylic adhesive interfaces. *Langmuir* **23**, 6966–6974 (2007).
31. C. Dhong, J. Fréchette, Coupled effects of applied load and surface structure on the viscous forces during peeling. *Soft Matter* **11**, 1901–1910 (2015).
32. C. Dhong, L. V. Kayser, R. Arroyo, A. Shin, M. Finn III, A. T. Kleinschmidt, D. J. Lipomi, Role of fingerprint-inspired relief structures in elastomeric slabs for detecting frictional differences arising from surface monolayers. *Soft Matter* **14**, 7483–7491 (2018).
33. K. Autumn, M. Sitti, Y. A. Liang, A. M. Peattie, W. R. Hansen, S. Sponberg, T. W. Kenny, R. Fearing, J. N. Israelachvili, R. J. Full, Evidence for van der Waals adhesion in gecko setae. *Proc. Natl. Acad. Sci. U.S.A* **99**, 12252–12256 (2002).
34. M. Janko, M. Wiertlewski, Y. Visell, Contact geometry and mechanics predict friction forces during tactile surface exploration. *Sci. Rep.* **8**, 4868 (2018).
35. M. Gellis, R. Pool, Two-point discrimination distances in the normal hand and forearm: Application to various methods of fingertip reconstruction. *Plast. Reconstr. Surg.* **59**, 57–63 (1977).
36. A. Oláh, H. Hillborg, G. J. Vancso, Hydrophobic recovery of UV/ozone treated poly (dimethylsiloxane): Adhesion studies by contact mechanics and mechanism of surface modification. *Appl. Surf. Sci.* **239**, 410–423 (2005).
37. B. Dzidek, S. Bochereau, S. A. Johnson, V. Hayward, M. J. Adams, Why pens have rubbery grips. *Proc. Natl. Acad. Sci. U.S.A* **114**, 10864–10869 (2017).
38. S. Gupta, J. G. Gonzalez, K. J. Loh, Self-sensing concrete enabled by nano-engineered cement-aggregate interfaces. *Struct. Health Monit.* **16**, 309–323 (2017).
39. E. K. Dimitriadis, F. Horkay, J. Maresca, B. Kachar, R. S. Chadwick, Determination of elastic moduli of thin layers of soft material using the atomic force microscope. *Biophys. J.* **82**, 2798–2810 (2002).
40. D. J. Navarick, E. Fantino, Stochastic transitivity and unidimensional behavior theories. *Psychol. Rev.* **81**, 426–441 (1974).
41. R. D. Luce, The choice axiom after twenty years. *J. Math. Psychol.* **15**, 215–233 (1977).
42. K. P. Burnham, D. R. Anderson, Multimodel inference: Understanding AIC and BIC in model selection. *Sociol. Methods Res.* **33**, 261–304 (2004).
43. M. D. Fairchild, *Color Appearance Models* (John Wiley & Sons, 2013).
44. R. Kohavi, A study of cross-validation and bootstrap for accuracy estimation and model selection, in *Ijcai* (Montreal, Canada, 1995), vol. 14, pp. 1137–1145.
45. M. Paré, A. M. Smith, F. L. Rice, Distribution and terminal arborizations of cutaneous mechanoreceptors in the glabrous finger pads of the monkey. *J. Comp. Neurol.* **445**, 347–359 (2002).
46. A. C. Grant, M. C. Thiagarajah, K. Sathian, Tactile perception in blind Braille readers: A psychophysical study of acuity and hyperacuity using gratings and dot patterns. *Percept. Psychophys.* **62**, 301–312 (2000).
47. G. Westheimer, S. P. McKee, Spatial configurations for visual hyperacuity. *Vision Res.* **17**, 941–947 (1977).

Acknowledgments: The study was approved by the IRB of the University of California, San Diego in accordance with the requirements of the Code of Federal Regulations on the Protection of Human Subjects (45 CFR 46 and 21 CFR 50 and 56), project #170248S. Data were collected from a total of 15 healthy volunteers between the ages of 19 and 31.
Funding: We are grateful for financial support through the NIH Director's New Innovator Award (grant no. 1DP2EB022358 to D.J.L.). S.G. and K.J.L. acknowledge support from the Office of

Naval Research (grant no. N00014-18-1-2483). **Author contributions:** C.D.: Conceptualization, investigation, formal analysis, and writing. R.M.: Investigation and writing. N.B.R.: Methodology and formal analysis. S.G.: Investigation. C.W.C.: Methodology. K.J.L.: Supervision. V.S.R.: Supervision. D.J.L.: Supervision and writing. L.V.K.: Investigation, formal analysis, and writing. All authors reviewed the manuscript. **Competing interests:** All authors declare that they have no competing interests. **Data and materials availability:** All data needed to evaluate the conclusions in the paper are present in the paper and/or the Supplementary Materials. Additional data related to this paper may be requested from the authors.

Submitted 1 February 2019
Accepted 23 July 2019
Published 30 August 2019
10.1126/sciadv.aaw8845

Citation: C. Dhong, R. Miller, N. B. Root, S. Gupta, L. V. Kayser, C. W. Carpenter, K. J. Loh, V. S. Ramachandran, D. J. Lipomi, Role of indentation depth and contact area on human perception of softness for haptic interfaces. *Sci. Adv.* **5**, eaaw8845 (2019).